Berberine inhibits excessive autophagy and protects myocardium against ischemia/reperfusion injury via the RhoE/AMPK pathway

FAJIA HU[1*], TIE HU[1*], YAMEI QIAO[2*], HUANG HUANG[3], ZEYU ZHANG[4], WENXIONG HUANG[3], JICHUN LIU[1] and SONGQING LAI[3]

[1]Department of Cardiovascular Surgery, The Second Affiliated Hospital, Jiangxi Medical College, Nanchang University; [2]School of Pharmacy, Jiangxi Medical College, Nanchang University; [3]Institute of Cardiovascular Surgical Diseases, The First Affiliated Hospital, Jiangxi Medical College, Nanchang University; [4]Institute of Nanchang University Trauma Medicine, The First Affiliated Hospital, Jiangxi Medical College, Nanchang University, Nanchang, Jiangxi 330006, P.R. China

Received December 19, 2023; Accepted March 20, 2024

DOI: 10.3892/ijmm.2024.5373

Abstract. Several studies have shown that berberine (BBR) is effective in protecting against myocardial ischemia-reperfusion injury (MI/RI). However, the precise molecular mechanism remains elusive. The present study observed the mechanism and the safeguarding effect of BBR against hypoxia/reoxygenation (H/R) myocardial injury in H9c2 cells. BBR pretreatment significantly improved the decrease of cell viability, P62 protein, Rho Family GTPase 3 (RhoE) protein, ubiquinone subunit B8 protein, ubiquinol-cytochrome *c* reductase core protein U, the Bcl-2-associated X protein/B-cell lymphoma 2 ratio, glutathione (GSH) and the GSH/glutathione disulphide (GSSG) ratio induced by H/R, while reducing the increase in lactate dehydrogenase, microtubule-associated protein 1 light 3 protein, caspase-3 activity, reactive oxygen species, GSSG and malonaldehyde caused by H/R. Transmission electron microscopy and LysoTracker Red DND-99 staining results showed that BBR pretreatment inhibited H/R-induced excessive autophagy by mediating RhoE. BBR also inhibited mitochondrial permeability transition, maintained the stability of the mitochondrial membrane potential, reduced the apoptotic rate, and increased the level of caspase-3. However, the protective effects of BBR were attenuated by pAD/RhoE-small hairpin RNA, rapamycin (an autophagy activator) and compound C (an AMP-activated protein kinase inhibitor). These new findings suggested that BBR protects the myocardium from MI/RI by inhibiting excessive autophagy, maintaining mitochondrial function, improving the energy supply and redox homeostasis, and attenuating apoptosis through the RhoE/AMP-activated protein kinase pathway.

Correspondence to: Dr Songqing Lai, Institute of Cardiovascular Surgical Diseases, The First Affiliated Hospital, Jiangxi Medical College, Nanchang University, 17 Yongwai Road, Nanchang, Jiangxi 330006, P.R. China
E-mail: ndyfy03743@ncu.edu.cn

Professor Jichun Liu, Department of Cardiovascular Surgery, The Second Affiliated Hospital, Jiangxi Medical College, Nanchang University, 1 Minde Road, Nanchang, Jiangxi 330006, P.R. China
E-mail: liujichun999@yeah.net

*Contributed equally

Key words: berberine, myocardium, ischemia/reperfusion injury, autophagy, RhoE/AMPK pathway

Introduction

Insufficient blood supply to the myocardium, known as acute myocardial injury, is a highly prevalent and fatal condition that poses a significant risk to human well-being (1). Therefore, the timely restoration of blood flow (reperfusion) remains the foundation of all current treatments to salvage ischemic myocardium (2). Research has indicated that myocardial ischemia reperfusion injury (MI/RI) can trigger different forms of regulated cell death (RCD), including apoptosis, ferroptosis and autophagy-induced cell death (3). Growing evidence indicates that autophagy could have both positive and negative effects on numerous diseases (4). Likewise, autophagy can have various impacts on MI/RI. While it can protect the myocardium during ischemia, an excessive amount of autophagy can harm the heart during reperfusion (5). The molecular mechanisms involved in MI/RI are complex, with factors such as mitochondrial abnormalities, oxidative stress and the generation of reactive oxygen species (ROS) playing a role (6-8).

Rho Family GTPase 3 (RhoE), also referred to as the Rnd3 protein, belongs to the Rho-GTPase group and controls the movement of the actin cytoskeleton, cell cycle advancement and programmed cell death (9). A previous study revealed that RhoE influences inflammation following myocardial infarction and promotes the recovery of the injured heart (10). A previous study revealed that RhoE could target and regulate gastric cancer proliferation through chaperone-mediated autophagy (11). However, its role in myocardial injury induced by MI/RI has not yet been investigated.

Berberine (BBR; PubChem ID: 2353) is an isoquinoline alkaloid obtained from herbaceous plants of the *Coptis* genus native to the Orient (12). A previous study reported

that BBR inhibits autophagy protecting the myocardium from MI/RI (13). However, the exact molecular mechanism by which BBR inhibits autophagy and whether BBR inhibits autophagy through RhoE/AMP-activated protein kinase (AMPK) remains unknown. BBR demonstrated the ability to decrease apoptosis in myocardial cells and enhance the compromised mechanical performance of the heart in an MI/RI model (14). Thus, the impact of BBR on mitigating MI/RI and its potential ability to prevent injury involving the RhoE/AMPK, were examined.

In the present study, a hypoxia/reoxygenation (H/R) injury model in H9c2 cells and a MI/RI injury model in mice were employed to: i) Confirm whether MI/RI injury induces excessive autophagy, which causes damage to the myocardium; ii) investigate whether BBR inhibits excessive autophagy induced by MI/RI; iii) investigate whether the RhoE/AMPK pathway mediates the inhibition of myocardial excessive autophagy by BBR; and iv) determine whether the cardioprotective benefits of BBR protective effects are linked to the apoptosis inhibition, oxidative stress suppression, energy metabolism enhancement and the maintenance of mitochondrial function.

Materials and methods

Materials and animals. BBR (with a purity exceeding 98%) was provided from Chengdu Must Bio-Technology Co., Ltd. Adenovirus pAd/RhoE-small hairpin (sh)RNA was sourced from Shanghai GenePharma Co., Ltd. Compound C and rapamycin (CC; cat. no. HY-13418A and Rap; cat. no. HY-10219) were purchased from MedChemExpress. The antibodies against NADH-ubiquinone oxidoreductase subunit B8 (NDUFB8; cat. no. R383060), ubiquinol-cytochrome *c* reductase core protein 2 (UQCRC2; cat. no. R382096), Bcl-2-associated X protein (Bax; cat. no. 380709), B-cell lymphoma 2 (Bcl-2; cat. no. 250198), phosphorylated (p-)AMP-activated protein kinase (p-AMPK; cat. no. 381164) and microtubule-associated protein 1 light 3 (LC3; cat. no. 350140) were obtained from Chengdu Zen-Bioscience Co., Ltd. (http://www.zen-bio.cn/). The antibodies AMP-activated protein kinase (AMPK; cat. no. 10929-2-AP) and anti-β-actin (cat. no. 66009-1-Ig) were purchased from Proteintech Group, Inc. Anti-RhoE (cat. no. YN1227) and anti-P62 (cat. no. YT7058) antibodies were supplied by ImmunoWay Biotechnology Company. Mouse and rabbit secondary antibodies (cat. nos. 511103 and 511203, respectively) were provided by Chengdu Zen-Bioscience Co., Ltd. 3-Methyladenine (3-MA; cat. no. HY-19312), an autophagic inhibitor, was bought from MedChem Express. Dimethyl sulfoxide (DMSO; cat. no. HY-Y0320) was obtained from MedChem Express.

A total of 30 healthy male C57BL/6 mice (6-8 weeks-old), weighing ~20 g, were supplied by the Animal Center of Nanchang University (Nanchang, China). The experimental procedure adhered to the guidelines of the National Institutes of Health (NIH) and was authorized by the Animal Experimentation Ethics Committee of The First Affiliated Hospital of Nanchang University (approval no. CDYFY-IACUC-202209QR004). The mice were housed under controlled conditions, including a temperature of 23±1˚C, humidity ranging between 40-50%, a 12-h light/dark cycle, and access to food and water *ad libitum*.

The animal was euthanized in case-predefined humane endpoints. These include: i) Weight loss: Rapid loss of 15-20% of original body weight; ii) weakness: Unable to eat and drink on his own, unable to stand for up to 24 h or unable to stand with extreme reluctance; and iii) the animal exhibits depression and hypothermia (<37˚C) without anesthesia or sedation. No mice showed abnormal signs of humanitarian endpoints throughout the experiment.

In vitro experiments

Cell culture. The H9c2 cell line was acquired from the Cell Bank/Stem Cell Bank located in Beijing, China. The cells were cultured in high-glucose Dulbecco's modified Eagle's medium (H-DMEM; HyClone; Cytiva) with the addition of 10% fetal bovine serum (Gibco; Thermo Fisher Scientific, Inc.), 100 U/ml penicillin, and 100 μg/ml streptomycin (Wuhan Servicebio Technology Co., Ltd.). The cells were cultivated in a humid incubator at 37˚C, a humidity level of 95%, an oxygen concentration of 21%, and a CO_2 concentration of 5%.

Transfection of adenovirus and H/R modeling. The transfection of adenovirus pAD/RhoE-shRNA [multiplicity of infection (MOI): 80; target sense sequence: 5'-GCAGCC ACTTACATAGAAT-3'; antisense sequence: 5'-ATTCTA TGTAAGTGGCTGC-3'] into H9c2 cells was carried out in H-DMEM containing 10% FBS. The transfection efficiency was ~85% after 48 h under 95% O_2 and 5% CO_2 at 37˚C, and the following experiments were conducted.

The cells were cultured in anoxia solution (1.0 mM $CaCl_2$, 20 mM HEPES, 10 mM KCl, 1.2 mM $MgSO_4$, 98.5 mM NaCl, 0.9 mM NaH_2PO_4, 36 mM $NaHCO_3$ and 40 mM sodium lactate, at pH 6.8) for hypoxia and in reoxygenation solution (1.0 mM $CaCl_2$, 5.5 mM glucose, 20 mM HEPES, 5 mM KCl, 1.2 mM $MgSO_4$, 129.5 mM NaCl, 0.9 mM NaH_2PO_4, 20 mM $NaHCO_3$, at pH 7.4) for reoxygenation. The H9c2 cells were incubated in a sealed anoxic chamber at 37˚C with a gas mixture of 95% nitrogen and 5% carbon dioxide for 3 h in a Petri dish. Following that, the gas mixture was altered to contain 95% oxygen and 5% carbon dioxide for a duration of 2 h to cause H/R damage (15,16).

Experimental grouping. H9c2 cells were assigned randomly into eight different groups: i) control group; ii) H/R group: H9c2 cells exposed to H/R injury; iii) BBR + H/R group: H9c2 cells were treated with BBR at concentrations of 1.25, 2.5, 5, 10, 20 and 40 μM for 48 h before H/R injury; iv) BBR + pAd/RhoE-shRNA + H/R group: H9c2 cells transfected with pAd/RhoE-shRNA for 48 h and then pretreated with 20 μM BBR for an additional 48 h prior to H/R injury; v) pAd/RhoE-shRNA + H/R group: H9c2 cells transfected with pAd/RhoE-shRNA and incubated for 48 h prior to H/R injury; vi) BBR + Rap group + H/R group: H9c2 cells pretreated with 20 μM BBR and 100 nM Rap for 48 h prior to H/R injury; vii) BBR + 5 μM compound C + H/R group: H9c2 cells pretreated with 20 μM BBR for 48 h and 100 nM Rap for 24 h before H/R injury; and viii) 20 μM BBR + 5 mM 3-MA group: H9c2 cells pretreated with 5 mM 3-MA for 24 h before H/R injury.

Cell viability and lactate dehydrogenase (LDH) activity assay. Cell viability was evaluated by utilizing the Cell Counting Kit-8 (CCK-8; Good Laboratory Practice Bioscience; cat.

no. GK10001). Each well was incubated with 10 μl of CCK-8 reagent for 1 h at 37˚C, and the absorbance was measured at 450 nm. LDH (Beyotime Institute of Biotechnology; cat. no. C0016) concentrations were measured following the manufacturer's guidelines. A total of 120 μl of supernatant were received from each group and added to a new 96-well plate; then 60 μl of LDH assay working solution was added to each well, incubated at 25˚C (avoiding light) for 30 min, and the absorbance was measured at 490 nm.

Measurement of oxidative stress. To evaluate intracellular ROS generation, a ROS detection kit (Beyotime Institute of Biotechnology; cat. no. S0033S) was utilized. H9c2 cell cultures were treated with DCFH-DA at 37˚C for a duration of 20 min without any exposure to light. Inverted fluorescence microscopy (Olympus Corporation) was used to observe the levels of ROS in the cell populations of different experimental groups. Malondialdehyde (MDA), glutathione (GSH) and glutathione disulfide (GSSG), levels were measured in the supernatant of H9c2 cells in each group according to the instructions provided in the kit (Beyotime Institute of Biotechnology; cat. no. S0053). The GSH/GSSG ratio was determined.

Lyso tracker red staining. H9c2 cells were incubated with a working solution of 50 nM Lyso-Tracker Red (Beyotime Institute of Biotechnology; cat. no. C1046) to perform Lyso tracker red staining. Incubation was carried out at 37˚C for 20 min while avoiding exposure to light. The examination of the cells was performed using an inverted fluorescence microscope (Olympus Corporation).

Assessment of caspase-3 activity. The activity of caspase-3 was evaluated in accordance with the instructions provided in the caspase-3 activity assay kit (cat. no. C1115) from Beyotime Institute of Biotechnology. The combination of reaction buffer, cell group homogenate, and caspase-3 substrate was thoroughly mixed and subsequently added to 96-well plates. The mixture was incubated at 37˚C for 2 h. Following incubation, the absorbance was measured at a wavelength of 405 nm using a microplate reader (Thermo Fisher Scientific, Inc.). The concentration of each group of proteins was determined using the Bradford method. Finally, caspase-3 activity was calculated.

Flow cytometry assay. Mitochondrial permeability transition (mPTP), mitochondrial membrane potential (MMP), and apoptosis were measured using the mPTP assay kit (cat. no. BB-48122), the JC-1 MMP assay kit (cat. no. BB-4105), and the Annexin V-fluorescein isothiocyanate (V-FITC) Apoptosis assay Kit (cat. no. BB-4101) (BestBio; https://www.bestbio.com.cn/index.html), according to the manufacturer's instruction, respectively. For mPTP detection, the cell suspensions were incubated with BbcellProbe M61 as well as a quencher for 15 min at 37˚C in the dark, followed by centrifugation at 1,000 x g at room temperature for 5 min and washing. The level of mPTP was immediately determined using a Cytomics FC 500 flow cytometer [excitation (Ex)=488 nm, emission (Em)=558 nm] (Beckman Coulter, Inc.). MMP levels were determined by incubating H9c2 cardiomyocytes with JC-1 dye at 37˚C for 30 min in the dark, followed by centrifugation, washing, and detection using a Cytomics FC 500 flow cytometer [530/580 nm (red) and 485/530 nm (green)]. For the apoptosis assay, cell suspensions were incubated with 5 μl of membrane-bound protein V-FITC and 10 μl of propidium iodide for 20 min at 4˚C and the cells were analyzed using a Cytomics FC 500 flow cytometer (Ex=488 nm; Em=578 nm). NovoExpress (v.6.2; Agilent Technologies, Inc.) was used to analyze the flow cytometric data.

Transmission electron microscopy imaging. After treatment, cells were collected, fixed (incubated in 2% glutaraldehyde at 25˚C for 2 h), washed, dehydrated, embedded, sectioned and stained (staining with 2% uranyl acetate and 2.6% lead citrate at 37˚C for 8 min). The structure of autophagosome in H9c2 cells was examined using transmission electron microscopy (TEM; Hitachi 7800; Hitachi, Ltd.).

Western blot analysis. Total cellular proteins from H9c2 cells were hydrolyzed in RIPA lysis buffer (Beyotime Institute of Biotechnology). The concentration of proteins was determined using the BCA protein assay kit (Good Laboratory Practice Bioscience). Electrophoresis on a 10% or 12% SDS-PAGE gel was carried out to separate 20 μg of proteins, which were then transferred onto polyvinylidene fluoride membranes. After blocking, the membranes were probed with primary antibodies (diluted to 1:1,000) against RhoE, LC3B, P62, AMPK, p-AMPK, Bcl-2, Bax, NDUFB8, UQCRC2 and β-actin for an overnight incubation at 4˚C. Subsequently, the membranes were exposed to secondary antibodies conjugated with horseradish peroxidase (1:20,000) at room temperature for 1 h. The internal reference for normalization was β-actin. Protein bands were analyzed using ImageJ v1.5.3 software (National Institutes of Health).

In vivo experiments. Mice were re-separated into four groups: i) sham group, ii) sham + BBR group, iii) ischemia-reperfusion (I/R) group, iv) I/R + BBR group. The sham + BBR group and I/R + BBR group were intragastrically administered 40 mg/kg BBR for 3 weeks. Mice from both the sham and I/R groups received a saline solution. Following the induction of anesthesia using 3% isoflurane, mice were positioned supine and maintained under 1.5% isoflurane. Subsequently, a thoracotomy was performed at the fourth intercostal space, opening the pericardium to reveal the heart. Closure of the left anterior descending artery (LAD) was achieved with a 4-0 silk suture, and a snare was created by passing a short polyethylene tube through the suture ends. The snare was clamped against the heart surface to establish ischemia and released for reperfusion. Mice in the sham group underwent a procedure that was similar but did not include clamping of the LAD. The hearts of the mice experienced 60 min of ischemia followed by 24 h of reperfusion in order to model MI/RI *in vivo*.

Following reperfusion, the Vevo2100 imaging system (Visual Sonics, Inc.) was used to measure the left ventricular end diastolic diameter, left ventricular end-systolic diameter, left ventricular ejection fraction (LVEF), and left ventricular fractional shortening (LVFS) of the left ventricle in mice under anesthesia with 1.5% isoflurane, using 2-dimensional transthoracic echocardiography.

After collecting ~0.5 ml of blood from each group of anesthetized mice through cardiac puncture, serum was extracted

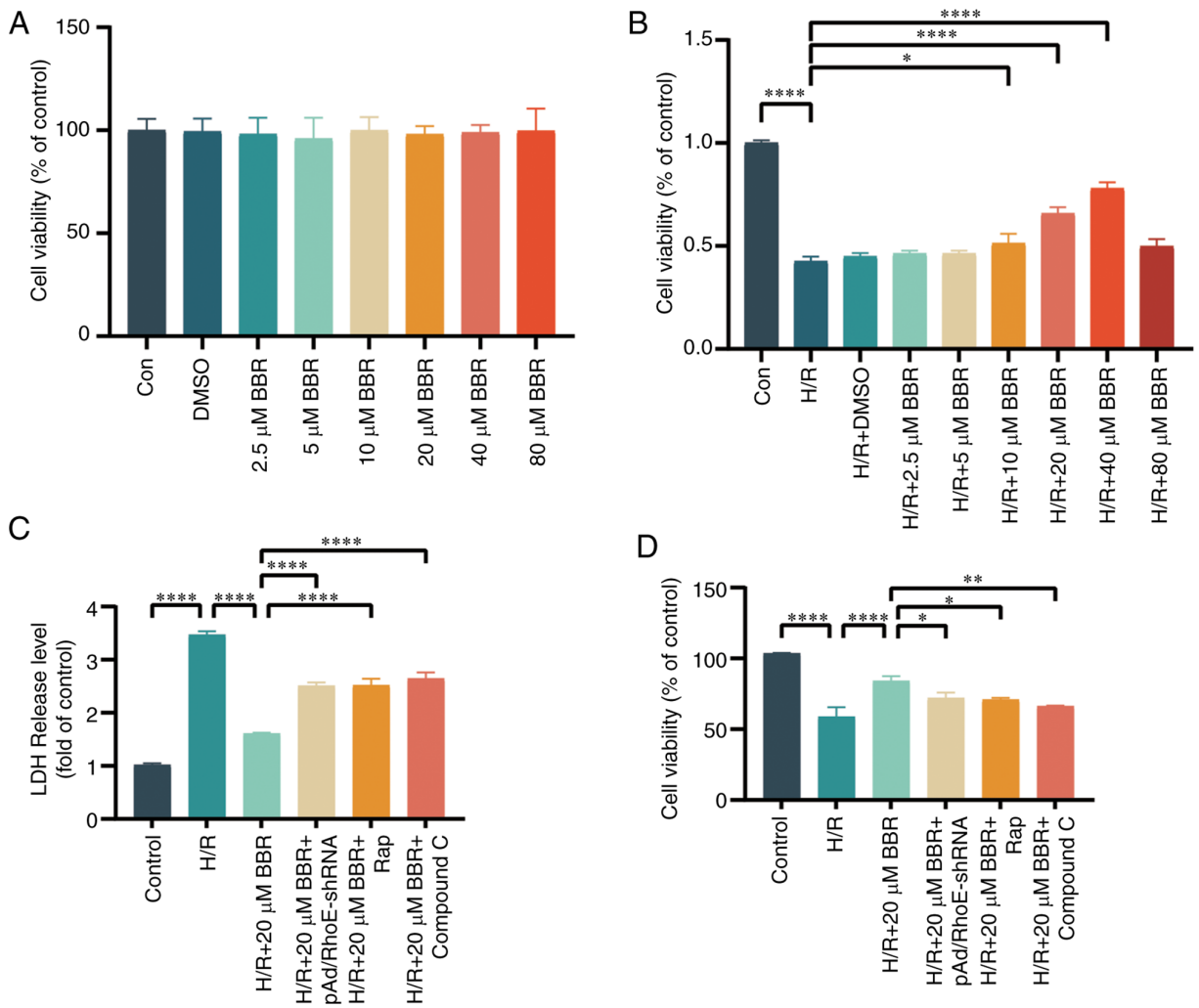

Figure 1. BBR protects to H9c2 cells from injury caused by H/R. (A) Histogram of CCK-8 detected the cell viability when the different concentrations of BBR were induced. (B) Histogram of CCK-8 detected the cell viability in H/R-induced cells after different concentrations of BBR. (C) Histogram of LDH activity in H/R-induced cells after treatment of each group separately. (D) Histogram of CCK-8 detected the cell viability in H/R-induced cells after treatment of each group separately. Data are expressed as the mean ± SD (n=3). *P<0.05, **P<0.01 and ****P<0.0001. BBR, berberine; H/R, hypoxia/reoxygenation; LDH, lactate dehydrogenase; Ad, adenovirus.

and prepared. Immediately after blood collection, the mice were euthanized with a 30% vol/min volumetric CO_2 displacement rate. The activities of serum LDH and creatine kinase (CK)-MB were then assessed. The myocardial infarct area was measured by triphenyl tetrazolium chloride staining, and the left ventricle was routinely fixed and sliced into 8 μM-thick sections, which were stained using Terminal Deoxynucleotidyl Transferase mediated dUTP Nick-End Labeling (TUNEL) and dihydroethidium (DHE) staining and visualized by light microscopy.

Statistical analysis. GraphPad Prism (Dotmatics) was utilized to conduct one-way analysis of variance (ANOVA) with Tukey post hoc analysis, with results being displayed as the mean ± standard deviation. P<0.05 was considered to indicate a statistically significant difference.

Results

BBR protects H9c2 cells from injury caused by H/R. An effective concentration of BBR was determined using the CCK-8 test. The survival of H9c2 cells was mostly unaffected after exposure to 0, 2.5, 5, 10, 20, 40, or 80 μM BBR or 1‰ DMSO. BBR enhanced cell survival in a dose-dependent manner but declined once it exceeded 80 μM. According to the principle of drug dosing, the ideal therapeutic level of a medication is typically above the level where it starts working and below the maximum safe concentration. Consequently, a 20 μM BBR concentration was utilized in following trials (Fig. 1A and B). A decrease in H9c2 cell viability post-H/R injury confirmed the successful establishment of the H/R injury model.

The effects of 20 μM BBR were significantly counteracted by pAD/RhoE-shRNA, 100 nM Rap (a substance that activates autophagy), and 5 μM compound C (a blocker of AMPK). The results indicated that BBR could protect H9c2 cells from H/R injury (Fig. 1C and D).

BBR inhibits autophagy by H/R-induced in H9c2 cells. The levels of RhoE and autophagy indicators were examined, such as P62 and the ratio of LC3-II to LC3-I, to evaluate the impact of BBR on the expression of RhoE and autophagy during H/R injury. Upon exposure to H/R, BBR enhanced the expression of RhoE

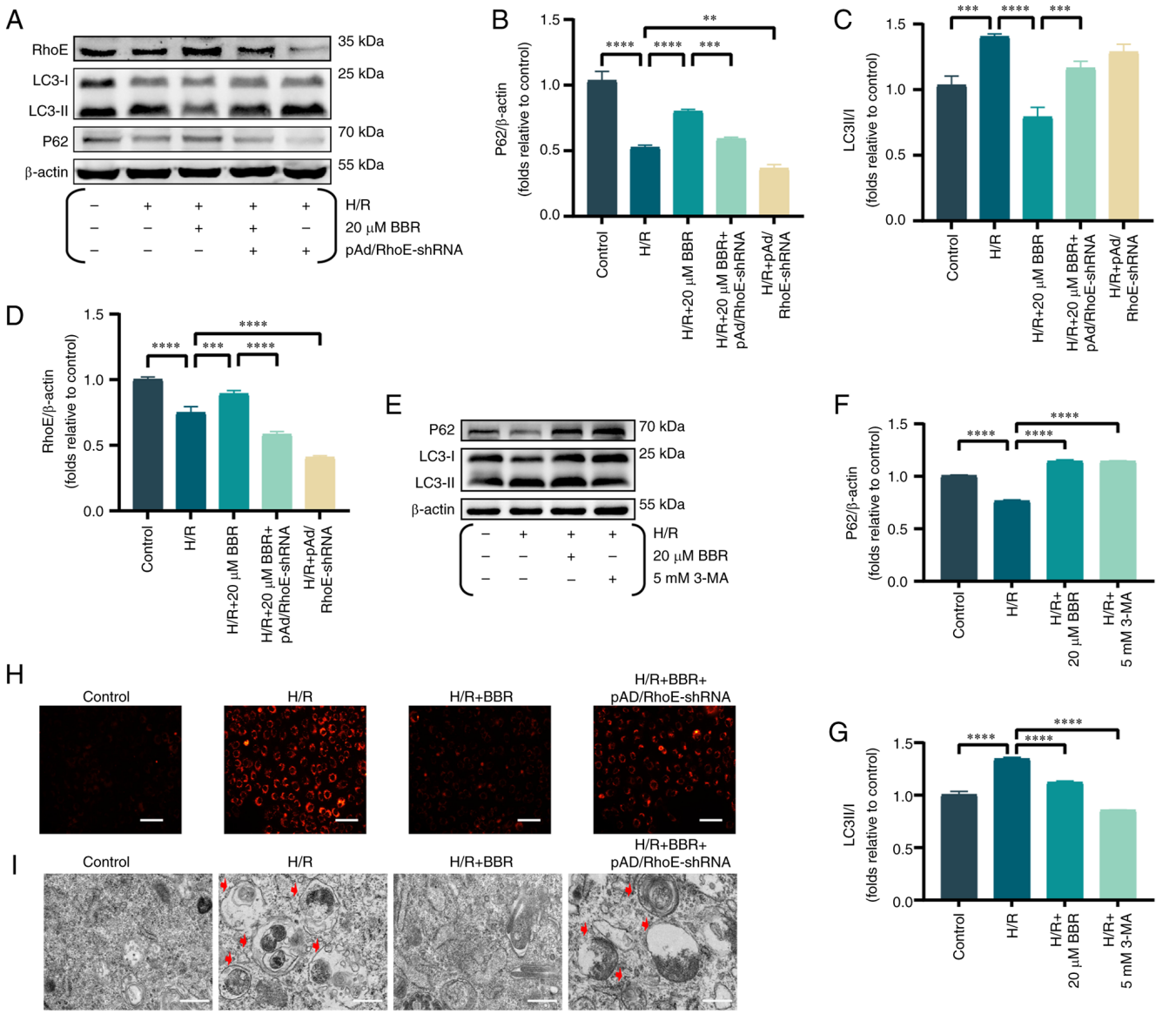

Figure 2. BBR inhibits autophagy by H/R-induced in H9c2 cells. (A) Western blot detection of RhoE protein, LC3 protein and P62 protein expression in H/R-induced cells after pretreatment with BBR, BBR + pAd/RhoE-shRNA and pAd/RhoE-shRNA. (B-D) Histogram of RhoE protein, LC3 protein and P62 protein expression. (E) Western blot detection of LC3 protein and P62 protein expression in H/R-induced cells after pretreatment with BBR and 3-MA. (F and G) Histogram of LC3 and P62 protein expression. (H) LysoTracker Red DND-99-stained images of H9c2 cells (magnification, x200; scale bar, 50 μm). (I) Transmission electron microscopy images of H9c2 cells (magnification, x6,000; scale bar, 1 μm). Data are expressed as the mean ± SD (n=3). **P<0.01, ***P<0.001 and ****P<0.0001. BBR, berberine H/R, hypoxia/reoxygenation; RhoE, Rho family GTPase 3; LC3, microtubule-associated protein 1 light 3; P62, Sequestosome 1; Ad, adenovirus; sh-, small hairpin; 3-MA, 3-Methyladenine.

and P62 while reducing the LC3-II/LC3-I ratio. Nevertheless, prior administration of pAd/RhoE-shRNA could reverse the expression of the aforementioned proteins (Fig. 2A-D).

The aforementioned effects of 20 μM BBR were simulated by adding 5 mM 3-MA (an autophagy inhibitor). The results showed that BBR had the same effect as the autophagy inhibitor 3-MA (Fig. 2E-G).

LysoTracker Red DND-99-stained H9c2 cells exhibited increased fluorescence intensity in the H/R group compared with the control group, suggesting that H/R induced autophagosome formation by decreasing lysosomal pH and enhancing autophagy. By contrast, BBR reduced the strong fluorescence in the H/R group and suppressed the formation of autophagosomes. pAd/RhoE-shRNA transfection ameliorated the aforementioned changes (Fig. 2H).

Transmission electron microscopy results revealed a rise in the number of autophagic vesicles in H9c2 cells within the H/R group. Additionally, pretreatment with BBR resulted in a reduction of autophagic vesicles, thereby inhibiting the autophagic process. The aforementioned Changes mentioned above could be reversed by pAd/RhoE-shRNA (Fig. 2I).

BBR inhibits excessive autophagy by H/R induced in H9c2 cells via the RhoE/AMPK pathway. Western blot analysis of AMPK protein phosphorylation was conducted to further examine the inhibitory impact of RhoE-mediated BBR on autophagy in the H/R injury model. BBR pretreatment significantly increased the levels of AMPK phosphorylation. However, pAd/RhoE-shRNA transfection only partially reversed the effects of BBR (Fig. 3A and B). The expression of p-AMPK, AMPK, P62

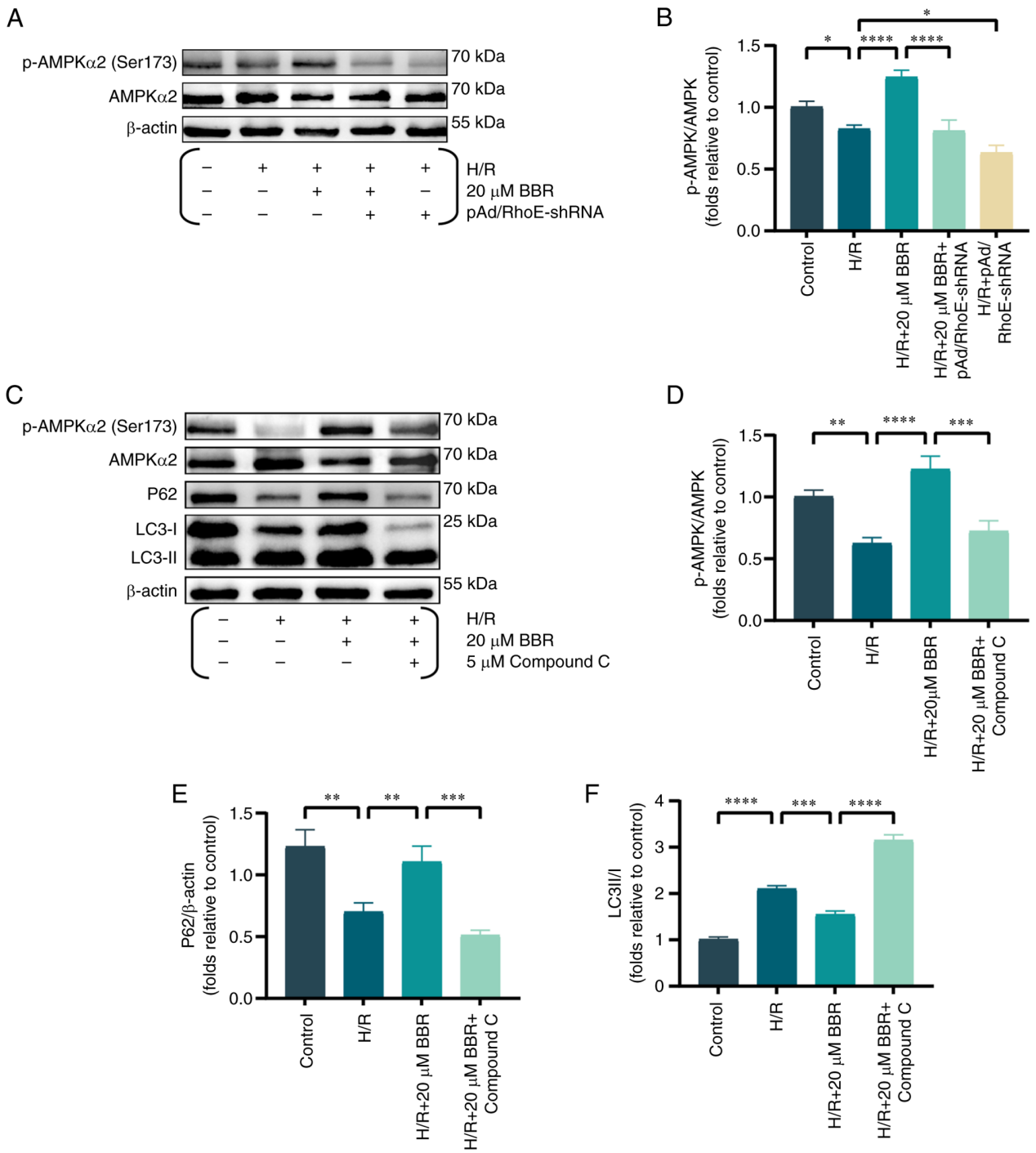

Figure 3. BBR inhibits excessive autophagy by H/R induced in H9c2 cells via the RhoE/Ampk pathway. (A) Western blot detection of p-AMPK protein and AMPK protein expression in H/R-induced cells after pretreatment with BBR, BBR + pAd/RhoE-shRNA and pAd/RhoE-shRNA. (B) Histogram of p-AMPK and AMPK protein ratios. (C) Western blot detection of p-AMPK, AMPK, LC3 and P62 protein expression in H/R-induced cells after pretreatment with BBR and BBR + Compound C. (D-F) Histogram of p-AMPK and AMPK protein ratios, LC3 and P62 protein expression. Data are expressed as the mean ± SD (n=3). *P<0.05, **P<0.01, ***P<0.001 and ****P<0.0001. BBR, berberine; H/R, hypoxia/reoxygenation; RhoE, Rho family GTPase 3; p-, phosphorylated; AMPK, AMP-activated protein kinase; Ad, adenovirus; sh, small hairpin; LC3, microtubule-associated protein 1 light 3; P62, Sequestosome 1.

and LC3 were analyzed in H9c2 cells, both with and without compound C (an AMPK inhibitor), to analyze the effects of the RhoE/AMPK pathway on BBR's protection against H/R damage. BBR enhanced the expression of P62 and the p-AMPK/AMPK ratio, while reducing the LC3-II/LC3-I ratio. Treatment with compound C nullified the impacts of BBR, indicating that the RhoE/AMPK pathway, which is associated with BBR, hindered the excessive autophagy induced by H/R (Fig. 3C-F).

BBR improves mitochondrial function in H9c2 cells after H/R injury. Mitochondria are recognized as the focal point of cellular energy metabolism, while the AMPK pathway serves as an energy detector that mirrors the state of the mitochondria. Previous studies verified a strong connection between mitochondrial impairment and MI/RI (17,18).

The energy supply of cardiomyocytes is maintained by the crucial involvement of mitochondrial electron transfer chain

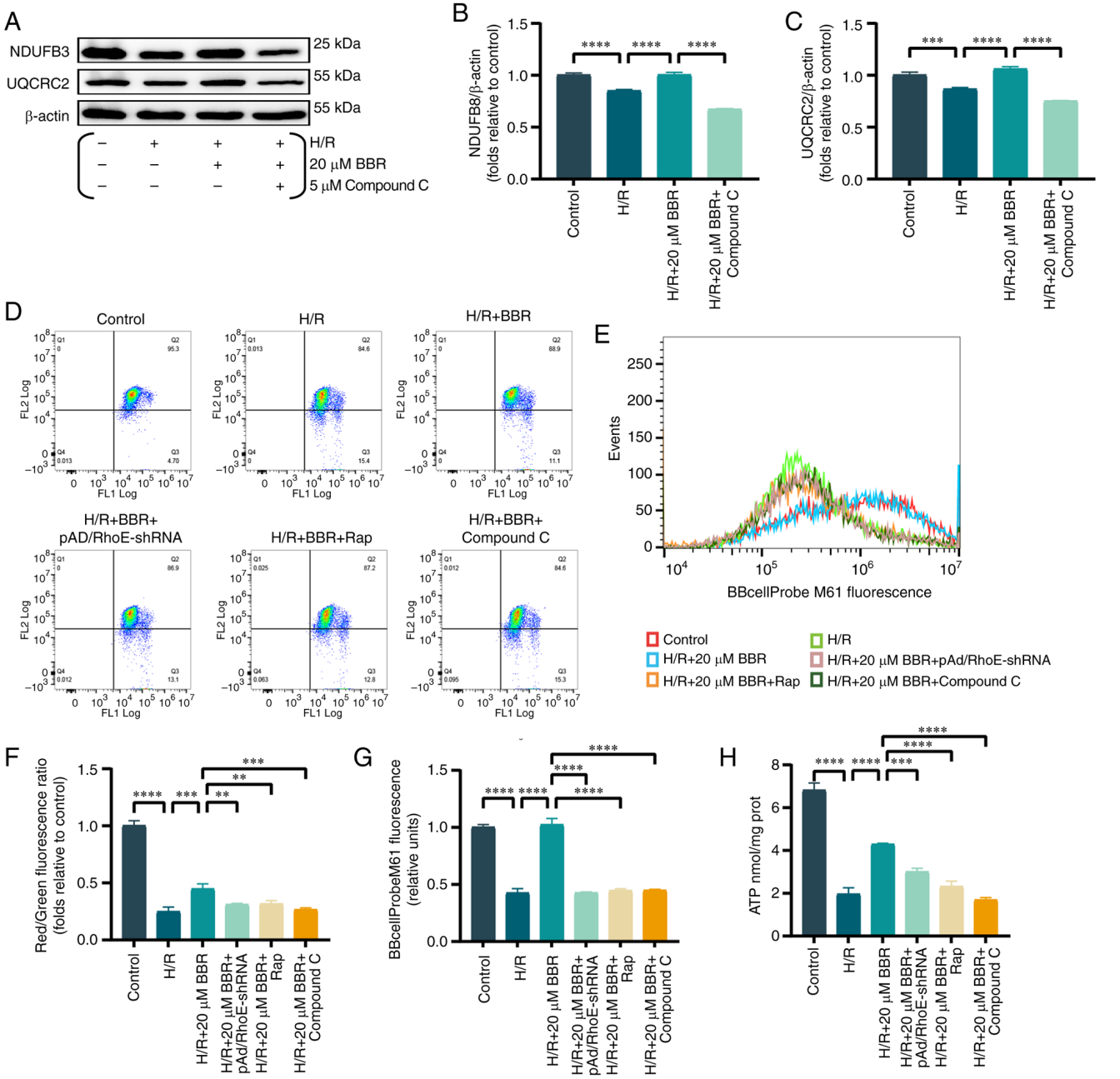

Figure 4. BBR improves mitochondrial function in H9c2 cells after H/R injury. (A) Western blot detection of NDUFB 8 and UQCRC 2 protein expression in H/R-induced cells after pretreatment with BBR and BBR + Compound C. (B and C) Histogram of NDUFB 8 and UQCRC 2 protein expression. (D) MMP levels detected by JC-1 in H9c2 cells by red/green fluorescence ratio. (E) Histogram of red/green fluorescence ratio. (F) Histogram of mPTP flow cytometry results. (G) Fluorescent probe BBcellProbe M61 indicating mPTP opening was detected by flow cytometry. (H) Histogram of ATP. Data are expressed as the mean ± SD (n=3). **P<0.01, ***P<0.001, ****P<0.0001. BBR, berberine; H/R, hypoxia/reoxygenation; NDUFB 8, Ubiquinone Oxidoreductase Subunit B8; UQCRC 2, Cytochrome b-c1 complex subunit 2, mitochondrial; MMP, mitochondrial membrane potential; mPTP, mitochondrial permeability transition; Ad, adenovirus.

complexes I and III (19). Consequently, the protein quantity of Ubiquinone Oxidoreductase Subunit B8 (NDUFB 8) (component of complex I) and Cytochrome b-c1 complex subunit 2, mitochondrial (UQCRC 2) component of complex III protein were analysed. BBR pretreatment rescued the downregulation of both levels in H/R-injured H9c2 cells compared with controls (Fig. 4A-C).

Similarly, MMP and abnormal opening of the mPTP are important judges of mitochondrial function. The mPTP assay and the MMP results revealed that the green fluorescence and the ratio of red/green fluorescence were significantly increased/decreased in the H/R group compared with the control group. Conversely, these effects were reversed in the H/R + BBR group. Notably, the protective effects of BBR pretreatment were eliminated in cells transfected with pAd/RhoE-shRNA and treated with Rap and compound C (Fig. 4D-G).

A reduction in ATP levels, which is the primary source of cellular energy, was observed following H/R damage. However, BBR pretreatment partially restored ATP levels. pAd/RhoE-shRNA, Rap and compound C reversed the aforementioned effects (Fig. 4H).

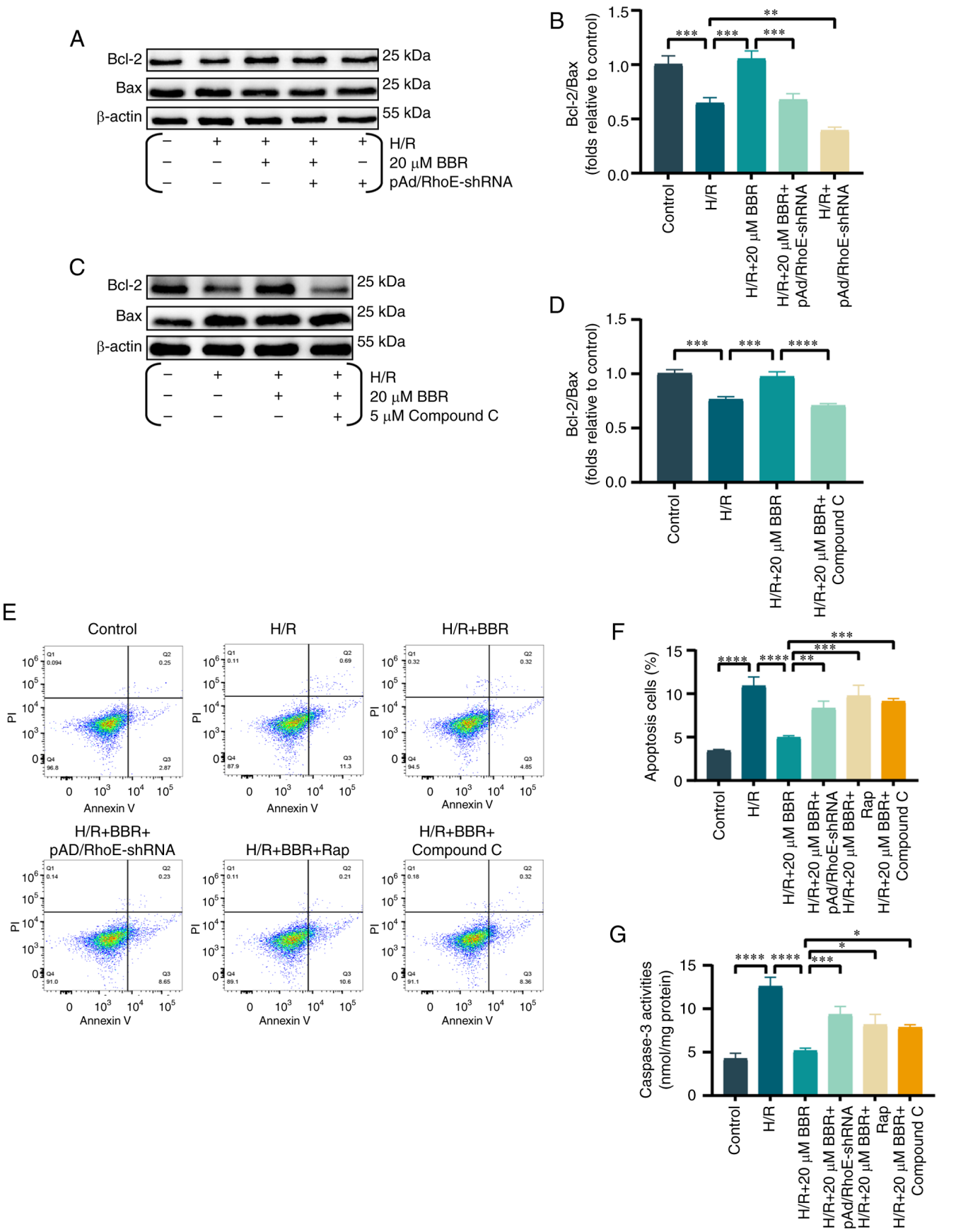

Figure 5. BBR attenuates apoptosis in H9c2 cells after H/R injury through the RhoE/AMPK pathways. (A) Western blot detection of Bcl-2 and Bax protein expression in H/R-induced cells after pretreatment with BBR, BBR + pAd/RhoE-shRNA and pAd/RhoE-shRNA (B) Histogram of Bcl-2 and Bax protein ratios. (C) Western blot detection of Bcl-2 and Bax protein expression in H/R-induced cells after pretreatment with BBR and BBR + Compound C. (D) Histogram of Bcl-2 and Bax protein ratios. (E) Apoptotic rate measured by Annexin V-FITC/PI detected by flow cytometry. (F) Histogram of apoptotic rate. (G) Histogram of caspase-3. Data are expressed as the mean ± SD (n=3). *P<0.05, **P<0.01, ***P<0.001 and ****P<0.0001. BBR, berberine; H/R, hypoxia/reoxygenation; RhoE, Rho family GTPase 3; AMPK, AMP-activated protein kinase; Ad, adenovirus; sh-, small hairpin.

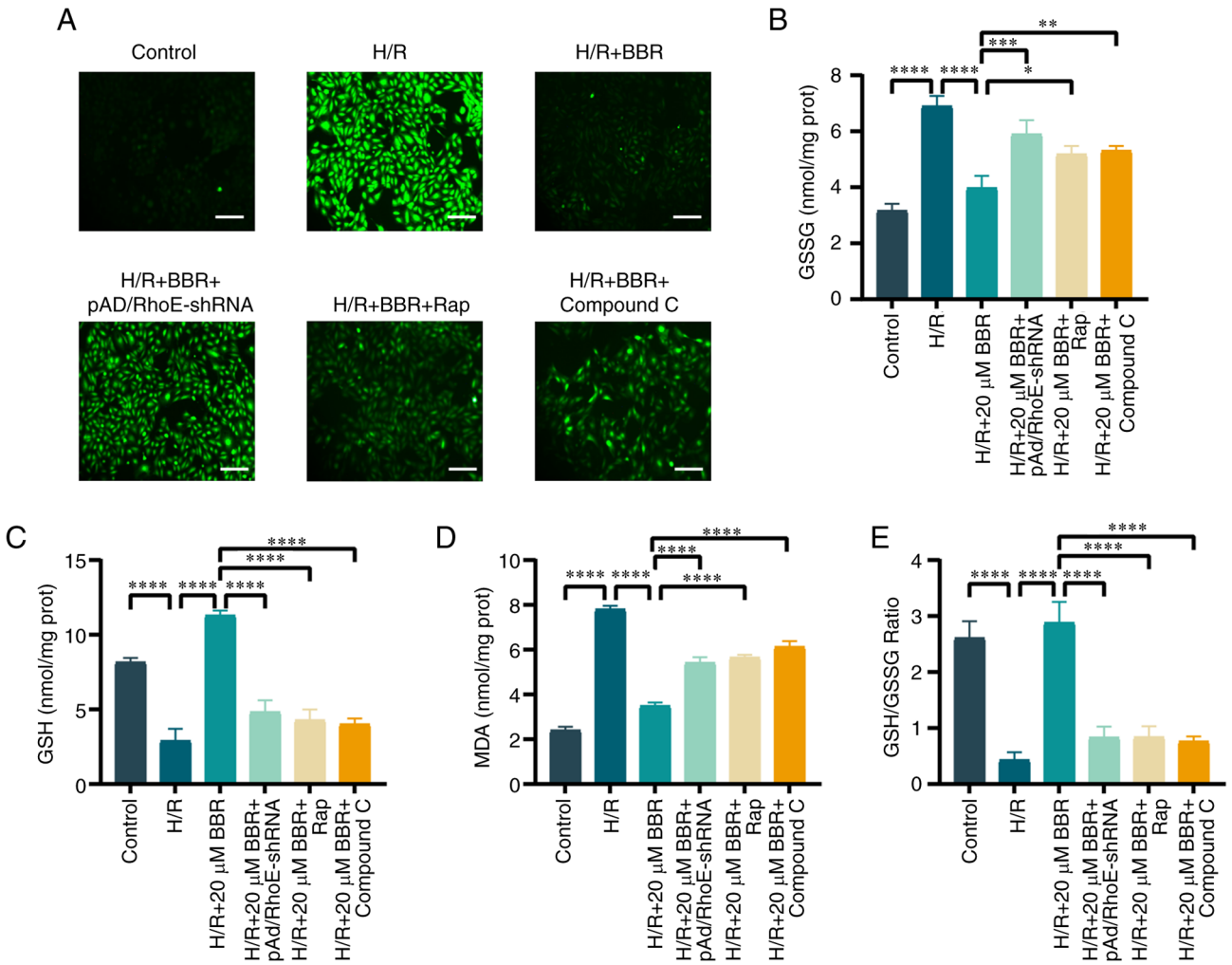

Figure 6. BBR inhibits oxidative stress by H/R induced in H9c2 cells. (A) DCFH-DA stained images for detection of ROS (magnification, x200; scale bar, 50 μm). (B) Histogram of GSH. (C) Histogram of GSSG. (D) Histogram of GSH and GSSG ratios. (E) Histogram of MDA. Data are expressed as the mean ± SD (n=3). *P<0.05, **P<0.01, ***P<0.001 and ****P<0.0001. BBR, berberine; H/R, hypoxia/reoxygenation; ROS, reactive oxygen species; GSH, glutathione; GSSG, glutathione disulfide; MDA, malondialdehyde; Ad, adenovirus.

The findings indicated that H/R has the potential to hinder mitochondrial function, while BBR has the ability to preserve mitochondrial function by suppressing excessive autophagy via the RhoE/AMPK pathway.

BBR attenuates apoptosis in H9c2 cells after H/R injury through the RhoE/AMPK pathways. Prior research indicated the significant involvement of apoptosis along with heightened autophagy in MI/RI injury (20). During the investigation into the suppression of excessive autophagy by BBR in H/R-damaged H9c2 cells, corresponding alterations were observed in apoptosis indicators. It was found that the ratio of Bcl-2/Bax ratio was decreased in H9c2 cells when exposed to H/R. However, the effect was prevented by pretreatment with BBR. The addition of pAd/RhoE-shRNA or compound C reversed these changes (Fig. 5A-D).

Similarly, apoptosis by flow cytometry was assayed and it was revealed that BBR inhibited H/R-mediated apoptosis and that pAd/RhoE-shRNA, Rap and compound c still abrogated the protective effect of BBR. The results suggested that BBR also inhibits apoptosis through the RhoE/AMPK pathway (Fig. 5E and F).

Caspase-3 levels were analyzed to study the effect of BBR on decreasing apoptosis in H9c2 cells following H/R injury via the RhoE/AMPK pathways (21), as caspase-3 is considered the main caspase involved in apoptosis execution. In the H/R group, there was an increase in caspase-3 activity, which was significantly reduced by BBR. However, pAd/RhoE-shRNA, Rap and compound C pretreatment all ameliorated the protective effects of BBR (Fig. 5G).

BBR inhibits oxidative stress by H/R induced in H9c2 cells. The generation of cellular ROS, and the levels of GSH, GSSG and MDA were investigated to illustrate the connection between the suppression of excessive autophagy and oxidative stress in H/R injury. BBR decreased the production within cells, replenished GSH levels and the ratio of GSH to GSSG, and lowered MDA and GSSG levels. The addition of pAd/RhoE-shRNA, Rap, or compound C prevented the protective effect of BBR against H/R injury in H9c2 cells (Fig. 6A-E). These results suggested that the inhibition of oxidative stress by BBR was RhoE/AMPK pathway-dependent and associated with the suppression of excessive autophagy.

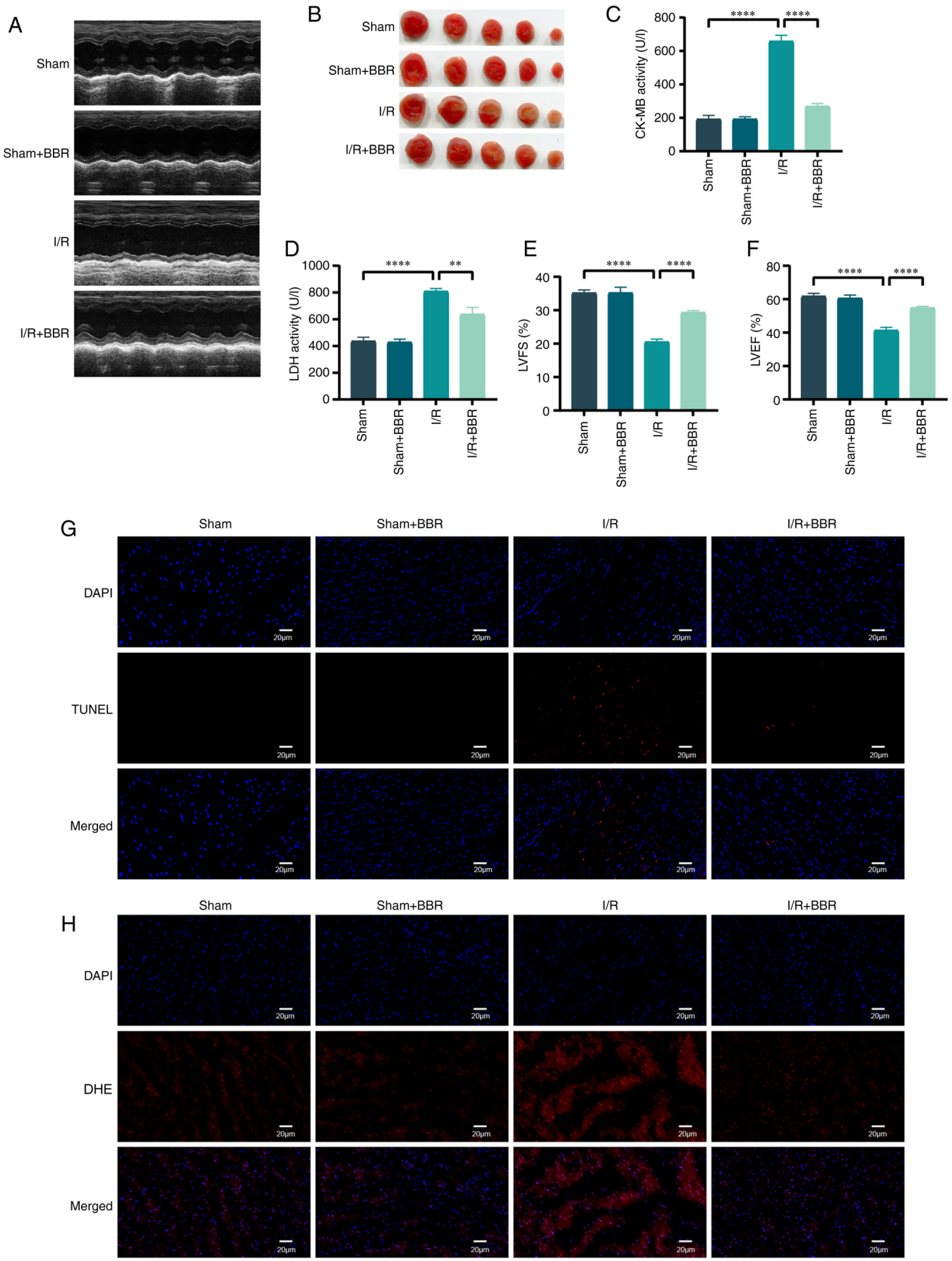

Figure 7. BBR protects mouse myocardium from I/R damage. (A) Echocardiographic images. (B) The image of the myocardium stained with TTC. (C) Histogram of LDH activity. (D) Histogram of CK activity. (E) Histogram of LVFS. (F) Histogram of LVEF. Data are expressed as the mean ± SD (n=6). **P<0.01 and ****P<0.0001. (G) The image of the myocardium was stained with TUNEL. (H) The image of the myocardium was stained with DHE. I/R, ischemia/reperfusion; LDH, lactate dehydrogenase; CK, creatine kinase; LVFS, left ventricular fractional shortening; LVEF, left ventricular ejection fraction; BBR, berberine.

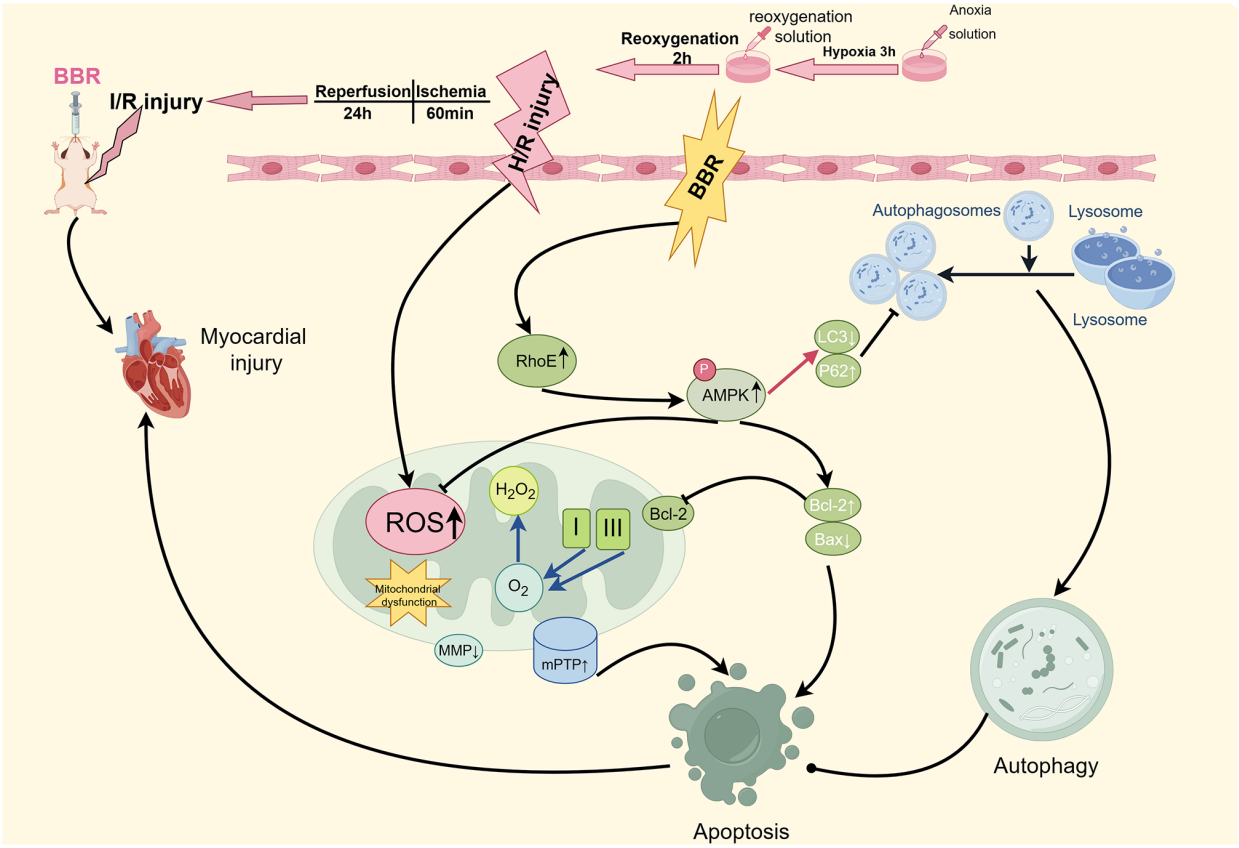

Figure 8. Schematic diagram of the mechanism by which BBR protects myocardium from I/R injury via the RhoE/AMPK pathway by Figdraw (https://www.figdraw.com). H/R, hypoxia/reoxygenation; BBR, berberine; I/R, ischemia reperfusion; RhoE, Rho family GTPase 3; AMPK, AMP-activated protein kinase; ROS, reactive oxygen species; MMP, mitochondrial membrane potential; mPTP, mitochondrial permeability transition.

BBR protects mouse myocardium from I/R damage. Male C57 BL/6 mice were utilized to simulate H/R injury in order to validate the protective impact of BBR *in vivo*. Mice afflicted with MI/RI injury exhibited significant elevation in serum LDH and CK-MB levels. The assessment of LV function in mice relied heavily on echocardiography. Post I/R injury, cardiac function suffered a severe decline manifested by decreased LVEF and LVFS. The administration of BBR (40 mg/kg) effectively restored these anomalous functional and enzymatic markers in I/R-induced injured mice (Fig. 7A and C-F). The infarct area was also notably increased, whereas the infarct area of I/R injury-induced mice treated with BBR was notably reduced (Fig. 7B). After I/R injury, TUNEL staining revealed numerous distinct TUNEL-positive cardiomyocytes and DHE staining demonstrated an increase in DHE intensity. TUNEL-positive cardiomyocytes and DHE-positive cells decreased after BBR treatment (Fig. 7G and H). By contrast, none of the aforementioned indexes changed significantly in the sham group after treatment with BBR (Fig. 7A-H).

Discussion

Autophagy serves as a cellular mechanism for survival, although uncontrolled autophagy can result in the demise of cells (22). Autophagy is often considered a double-edged sword in MI/RI. Moderate autophagy is beneficial for cardiomyocyte resistance to ischemia-reperfusion (23), but uncontrolled autophagy results in cardiomyocyte death (24). This moderate autophagy is usually called protective autophagy, while this uncontrolled autophagy is called excessive autophagy. In the present study, excessive autophagy during MI/RI severely damaged cardiomyocytes. However, to date, there are no studies on whether the cardioprotective effects of BBR are RhoE/AMPK pathway-dependent and which RCDs are involved in the protective process. The innovation of the present study lies in the fact that the myocardial protective effect of BBR was dependent on the RhoE/AMPK pathway, and various enzymatic and functional indices suggested that the apoptosis and autophagy mechanisms of RCD were involved in the pathologic process of MI/RI through. The H9c2 cell line was used in the present study because it can well mimic the response of primary cellular cardiomyocytes to hypoxia, and its energy metabolism pattern is similar to that of primary cardiomyocytes. However, the use of a single cell line is also a potential limitation to the present study.

BBR has been extensively utilized in the management of heart conditions (25). Numerous studies have reported that BBR improves MI/RI through various mechanisms, such as its antioxidant, anti-apoptotic, anti-inflammatory and endoplasmic reticulum stress properties (25-30). However, whether BBR can target multiple RCDs and whether the RhoE/AMPK pathway is involved is unclear. In a previous investigation, it was found that TSN pretreatment successfully reduced H9c2 cardiomyocyte damage in an H/R injury model by inhibiting apoptosis and ferroptosis (16). Therefore, drugs capable of targeting multiple RCDs are expected to be the best treatment

for MI/RI. In summary, it was hypothesized that BBR may also attenuate MI/RI by inhibiting different RCDs. It was found that along with RhoE/AMPK pathway activation, BBR significantly inhibited MI/RI-induced excessive autophagy. Notably, reducing RhoE expression, inhibiting the AMPK pathway or suppressing excessive autophagy greatly diminished the cardioprotective effects and inhibited excessive autophagy, providing evidence that the RhoE/AMPK pathway and the inhibition of excessive autophagy play a crucial role in the anti-MI/RI effects of BBR.

RhoE belongs to the RND subfamily in the RHO family (31). Earlier investigations have indicated that RhoE may function as a chaperone-mediated autophagy substrate implicated in controlling the proliferation of gastric cancer cells (11). Prior research by the authors revealed that RhoE regulates inflammation following myocardial infarction and facilitates the healing of the damaged heart (10). In the present study, it was revealed that RhoE not only participates in the protective effect of BBR on cardiomyocytes in MI/RI but it also has an important role in inhibiting excessive autophagy.

It has been previously indicated that the AMPK complex consists of three subunits: A catalytic α-subunit and two regulatory subunits, β and γ (32). Numerous prior investigations demonstrated that AMPK stimulation had the potential to enhance autophagy (33,34). However, recent research indicated that AMPK can impede autophagy in a photo-oxidative damage model, thereby providing substantial protection to photoreceptors against photo-oxidative damage (35). In addition, data from a study on heart failure suggested that AMPK could improve cardiac function by attenuating autophagy during the development of chronic heart failure, which may be related to mTORC2 activation and downstream effects (36). In the experiments performed in the present study, BBR triggered AMPK and protected cardiomyocytes by suppressing excessive autophagy in MI/RI. Remarkably, the introduction of the AMPK inhibitor compound C resulted in the restoration of certain autophagic flux. Numerous prior investigations similarly demonstrated that the inhibition of autophagy induced by AMPK activation might encompass the regulation of various signaling pathways, including the suppression of nuclear factor (NF)-κB signaling, the phosphorylation of ULK 1, or the inhibition of endoplasmic reticulum stress signaling (37,38). The inhibition of autophagy dependent on AMPK onset is also reliant on a particular form of stimulus or trauma and is intricately linked to the cellular energy status (39). Nevertheless, the specific molecular pathways still require further investigation.

As markers of autophagic flux, LC3 and P62 are often used to evaluate the level of autophagy. Activated LC3-I can be transferred to Atg3, which then binds phosphatidylethanolamine to carboxyglycine to produce treated LC3B-II (40-42). P62/SQSTM1 attaches to polyubiquitylated proteins and forms clumps via its ubiquitin-binding structural domain while also binding to LC3B-II through its LC3 interacting region to facilitate the breakdown of ubiquitylated protein clumps in autophagic lysosomes (43-45). In the present study, it was identified that P62 and LC3 displayed synchronized alterations, indicating that BBR preconditioning safeguards cardiomyocytes against MI/RI by restraining excessive autophagy. The inhibitory effect of BBR on autophagy in cardiomyocytes in MI/RI was nullified by pAd/RhoE-shRNA transfection or treatment with Rap, or compound C. TEM and the LysoTracker Red DND-99-stained observations demonstrated similar results.

Previously, various forms of cellular demise were considered to be unrelated to one another. However, advancements in molecular biology have led to a growing examination of their interconnected communication (46,47). Interactions between different autophagy-associated and apoptosis-associated proteins have been identified, and crosstalk between the two modes of cell death occurs at various stages of MI/RI development (48,49). The experiments of the present study revealed that BBR inhibited excessive autophagy while significantly reducing H/R-induced apoptosis in H9c2 cells, decreasing caspase-3 activity, and inducing an increase in the Bcl-2/Bax ratio. Of note, the effect of BBR on apoptosis-related indicators was prevented not only by the inclusion of pAd/RhoE-shRNA transfection or compound C treatment, but also by the inclusion of the autophagy stimulator Rap. These findings indicated that BBR has the ability to protect cardiomyocytes from MI/RI by suppressing excessive autophagy via the RhoE/AMPK pathway. Additionally, it can also impact apoptosis through the RhoE/AMPK pathway to prevent cardiomyocytes from MI/RI. The two modes of cell death were observed to be in correlated crosstalk. However, the specific proteins through which the crosstalk process is accomplished need to be further investigated.

Prior research has indicated that irregularities in MMP and the opening of mPTP are significant contributors to MI/RI (50,51). The opening of mPTP can decrease MMP, release of cytochrome *c*, decrease in ATP synthesis, and ultimately cause the death of cardiomyocytes (52).The results of the present study suggested that BBR inhibits oxidative stress, maintains mitochondrial function, and protects the myocardium from MI/RI. AMPK has additionally been discovered to be linked with energy metabolism, facilitating the oxidation of fatty acids and tricarboxylic acid cycling (53,54). The present study revealed that pre-treatment with BBR activated AMPKα2 and boosted energy production. Cardiomyocytes received an adequate energy supply, and resistance to MI/RI was enhanced. In summary, it was identified that MI/RI induces severe damage to cardiomyocytes by activating excessive autophagy. However, BBR can counteract this process by inhibiting autophagy, preserving mitochondrial function, enhancing energy supply, maintaining redox homeostasis, and reducing apoptosis via the RhoE/AMPK pathway. These effects ultimately protect the myocardium from MI/RI (Fig. 8).

Acknowledgements

Not applicable.

Funding

The present study was supported by the National Natural Science Foundation of China (grand nos. 82160073 and 82360057), the Jiangxi Provincial Natural Science Foundation (grant. nos. 20224ACB206002 and 20232BAB206009) and the Young Research and Cultivation Fund of the First Affiliated Hospital of Nanchang University (grant. no. YFYPY202128).

Availability of data and materials

The data generated in the present study may be requested from the corresponding author on reasonable request.

Authors' contributions

SL, JL and HH conceptualized, designed and administrated the present study. FH, TH and YQ performed cell experiments, animal experiments, data analysis and interpretation. ZZ and WH performed other cell experiments. SL and JL confirm the authenticity of all the raw data. All authors wrote the manuscript. All authors read and approved the final version of the manuscript.

Ethics approval and consent to participate

Animal experiments followed the guidelines of the National Institutes of Health and were authorized by the Animal Experimentation Ethics Committee of the First Affiliated Hospital of Nanchang University (Nanchang, China) (approval. no. CDYFY-IACUC-202209QR004).

Patient consent for publication

Not applicable.

Competing interests

The authors declare that they have no competing interests.

References

1. Heusch G: Myocardial ischaemia-reperfusion injury and cardioprotection in perspective. Nat Rev Cardiol 17: 773-789, 2020.
2. Wang K, Li Y, Qiang T, Chen J and Wang X: Role of epigenetic regulation in myocardial ischemia/reperfusion injury. Pharmacol Res 170: 105743, 2021.
3. Deng J: Advanced research on the regulated necrosis mechanism in myocardial ischemia-reperfusion injury. Int J Cardiol 334: 97-101, 2021.
4. Sciarretta S, Maejima Y, Zablocki D and Sadoshima J: The role of autophagy in the heart. Annu Rev Physiol 80: 1-26, 2018.
5. Dong Y, Chen H, Gao J, Liu Y, Li J and Wang J: Molecular machinery and interplay of apoptosis and autophagy in coronary heart disease. J Mol Cell Cardiol 136: 27-41, 2019.
6. Yu Y, Wang M, Chen R, Sun X, Sun G and Sun X: Gypenoside XVII protects against myocardial ischemia and reperfusion injury by inhibiting ER stress-induced mitochondrial injury. J Ginseng Res 45: 642-653, 2021.
7. Tie R, Ji L, Nan Y, Wang W, Liang X, Tian F, Xing W, Zhu M, Li R and Zhang H: Achyranthes bidentata polypeptides reduces oxidative stress and exerts protective effects against myocardial ischemic/reperfusion injury in rats. Int J Mol Sci 14: 19792-19804, 2013.
8. Pisarenko O, Shulzhenko V, Studneva I, Pelogeykina Y, Timoshin A, Anesia R, Valet P, Parini A and Kunduzova O: Structural apelin analogues: Mitochondrial ROS inhibition and cardiometabolic protection in myocardial ischaemia reperfusion injury. Br J Pharmacol 172: 2933-2945, 2015.
9. Jie W, Andrade KC, Lin X, Yang X, Yue X and Chang J: Pathophysiological functions of Rnd3/RhoE. Compr Physiol 6: 169-186, 2015.
10. Dai Y, Song J, Li W, Yang T, Yue X, Lin X, Yang X, Luo W, Guo J, Wang X, *et al*: RhoE fine-tunes inflammatory response in myocardial infarction. Circulation 139: 1185-1198, 2019.
11. Zhou J, Yang J, Fan X, Hu S, Zhou F, Dong J, Zhang S, Shang Y, Jiang X, Guo H, *et al*: Chaperone-mediated autophagy regulates proliferation by targeting RND3 in gastric cancer. Autophagy 12: 515-528, 2016.
12. Fang X, Wu H, Wei J, Miao R, Zhang Y and Tian J: Research progress on the pharmacological effects of berberine targeting mitochondria. Front Endocrinol (Lausanne) 13: 982145, 2022.
13. Wu X, Liu Z, Yu XY, Xu S and Luo J: Autophagy and cardiac diseases: Therapeutic potential of natural products. Med Res Rev 41: 314-341, 2021.
14. Yu L, Li F, Zhao G, Yang Y, Jin Z, Zhai M, Yu W, Zhao L, Chen W, Duan W and Yu S: Protective effect of berberine against myocardial ischemia reperfusion injury: Role of Notch1/Hes1-PTEN/Akt signaling. Apoptosis 20: 796-810, 2015.
15. Huang H, Lai S, Luo Y, Wan Q, Wu Q, Wan L, Qi W and Liu J: Nutritional preconditioning of apigenin alleviates myocardial ischemia/reperfusion injury via the mitochondrial pathway mediated by Notch1/Hes1. Oxid Med Cell Longev 2019: 7973098, 2019.
16. Hu T, Zou HX, Le SY, Wang YR, Qiao YM, Yuan Y, Liu JC, Lai SQ and Huang H: Tanshinone IIA confers protection against myocardial ischemia/reperfusion injury by inhibiting ferroptosis and apoptosis via VDAC1. Int J Mol Med 52: 109, 2023.
17. Cai CC, Zhu JH, Ye LX, Dai YY, Fang MC, Hu YY, Pan SL, Chen S, Li PJ, Fu XQ and Lin ZL: Glycine protects against hypoxic-ischemic brain injury by regulating mitochondria-mediated autophagy via the AMPK pathway. Oxid Med Cell Longev 2019: 4248529, 2019.
18. Chaudhary KR, Batchu SN, Das D, Suresh MR, Falck JR, Graves JP, Zeldin DC and Seubert JM: Role of B-type natriuretic peptide in epoxyeicosatrienoic acid-mediated improved post-ischaemic recovery of heart contractile function. Cardiovasc Res 83: 362-370, 2009.
19. Monzel AS, Enriquez JA and Picard M: Multifaceted mitochondria: Moving mitochondrial science beyond function and dysfunction. Nat Metab 5: 546-562, 2023.
20. Deng X, Ye F, Zeng L, Luo W, Tu S, Wang X and Zhang Z: Dexmedetomidine mitigates myocardial ischemia/reperfusion-induced mitochondrial apoptosis through targeting lncRNA HCP5. Am J Chin Med 50: 1529-1551, 2022.
21. Diao X, Wang J, Zhu H and He B: Overexpression of programmed cell death 5 in a mouse model of ovalbumin-induced allergic asthma. BMC Pulm Med 16: 149, 2016.
22. Willis MS, Min JN, Wang S, McDonough H, Lockyer P, Wadosky KM and Patterson C: Carboxyl terminus of Hsp70-interacting protein (CHIP) is required to modulate cardiac hypertrophy and attenuate autophagy during exercise. Cell Biochem Funct 31: 724-735, 2013.
23. Campos JC, Queliconi BB, Bozi LHM, Bechara LRG, Dourado PMM, Andres AM, Jannig PR, Gomes KMS, Zambelli VO, Rocha-Resende C, *et al*: Exercise reestablishes autophagic flux and mitochondrial quality control in heart failure. Autophagy 13: 1304-1317, 2017.
24. Bitirim CV, Ozer ZB, Aydos D, Genc K, Demirsoy S, Akcali KC and Turan B: Cardioprotective effect of extracellular vesicles derived from ticagrelor-pretreated cardiomyocyte on hyperglycemic cardiomyocytes through alleviation of oxidative and endoplasmic reticulum stress. Sci Rep 12: 5651, 2022.
25. Fu L, Chen W, Guo W, Wang J, Tian Y, Shi D, Zhang X, Qiu H, Xiao X, Kang T, *et al*: Berberine targets AP-2/hTERT, NF-κB/COX-2, HIF-1α/VEGF and cytochrome-c/caspase signaling to suppress human cancer cell growth. PLoS One 8: e69240, 2013.
26. Liu DQ, Chen SP, Sun J, Wang XM, Chen N, Zhou YQ, Tian YK and Ye DW: Berberine protects against ischemia-reperfusion injury: A review of evidence from animal models and clinical studies. Pharmacol Res 148: 104385, 2019.
27. Zhao L, Li H, Gao Q, Xu J, Zhu Y, Zhai M, Zhang P, Shen N, Di Y, Wang J, *et al*: Berberine attenuates cerebral ischemia-reperfusion injury induced neuronal apoptosis by down-regulating the CNPY2 signaling pathway. Front Pharmacol 12: 609693, 2021.
28. Zhu JR, Lu HD, Guo C, Fang WR, Zhao HD, Zhou JS, Wang F, Zhao YL, Li YM, Zhang YD, *et al*: Berberine attenuates ischemia-reperfusion injury through inhibiting HMGB1 release and NF-κB nuclear translocation. Acta Pharmacol Sin 39: 1706-1715, 2018.
29. Yang J, Yan H, Li S and Zhang M: Berberine ameliorates MCAO induced cerebral ischemia/reperfusion injury via activation of the BDNF-TrkB-PI3K/Akt signaling pathway. Neurochem Res 43: 702-710, 2018.
30. Chen C, Lin Q, Zhu XY, Xia J, Mao T, Chi T, Wan J, Lu JJ, Li Y, Cui J, *et al*: Pre-clinical evidence: Berberine as a promising cardioprotective candidate for myocardial ischemia/reperfusion injury, a systematic review, and meta-analysis. Front Cardiovasc Med 8: 646306, 2021.

31. Endzhievskaya S, Hsu CK, Yang HS, Huang HY, Lin YC, Hong YK, Lee JYW, Onoufriadis A, Takeichi T, Yu-Yun Lee J, *et al*: Loss of RhoE function in dermatofibroma promotes disorganized dermal fibroblast extracellular matrix and increased integrin activation. J Invest Dermatol 143: 1487-1497.e9, 2023.
32. Herzig S and Shaw RJ: AMPK: Guardian of metabolism and mitochondrial homeostasis. Nat Rev Mol Cell Biol 19: 121-135, 2018.
33. Zhuang A, Chai P, Wang S, Zuo S, Yu J, Jia S, Ge S, Jia R, Zhou Y, Shi W, *et al*: Metformin promotes histone deacetylation of optineurin and suppresses tumour growth through autophagy inhibition in ocular melanoma. Clin Transl Med 12: e660, 2022.
34. Kim TW, Cheon C and Ko SG: SH003 activates autophagic cell death by activating ATF4 and inhibiting G9a under hypoxia in gastric cancer cells. Cell Death Dis 11: 717, 2020.
35. Li YL, Zhang TZ, Han LK, He C, Pan YR, Fan B and Li GY: The AMPK-dependent inhibition of autophagy plays a crucial role in protecting photoreceptor from photooxidative injury. J Photochem Photobiol B 245: 112735, 2023.
36. Li Y, Wang Y, Zou M, Chen C, Chen Y, Xue R, Dong Y and Liu C: AMPK blunts chronic heart failure by inhibiting autophagy. Biosci Rep 38: BSR20170982, 2018.
37. Lu G, Wu Z, Shang J, Xie Z, Chen C and Zhang C: The effects of metformin on autophagy. Biomed Pharmacother 137: 111286, 2021.
38. Nwadike C, Williamson LE, Gallagher LE, Guan JL and Chan EYW: AMPK inhibits ULK1-dependent autophagosome formation and lysosomal acidification via distinct mechanisms. Mol Cell Biol 38: e00023-18, 2018.
39. He H, Wang L, Qiao Y, Yang B, Yin D and He M: Epigallocatechin-3-gallate pretreatment alleviates doxorubicin-induced ferroptosis and cardiotoxicity by upregulating AMPKα2 and activating adaptive autophagy. Redox Biol 48: 102185, 2021.
40. Parzych KR and Klionsky DJ: An overview of autophagy: Morphology, mechanism, and regulation. Antioxid Redox Signal 20: 460-473, 2014.
41. Glick D, Barth S and Macleod KF: Autophagy: Cellular and molecular mechanisms. J Pathol 221: 3-12, 2010.
42. Mizushima N and Komatsu M: Autophagy: Renovation of cells and tissues. Cell 147: 728-741, 2011.
43. Lamark T, Svenning S and Johansen T: Regulation of selective autophagy: The p62/SQSTM1 paradigm. Essays Biochem 61: 609-624, 2017.
44. Jeong SJ, Zhang X, Rodriguez-Velez A, Evans TD and Razani B: p62/SQSTM1 and selective autophagy in cardiometabolic diseases. Antioxid Redox Signal 31: 458-471, 2019.
45. Deng Z, Lim J, Wang Q, Purtell K, Wu S, Palomo GM, Tan H, Manfredi G, Zhao Y, Peng J, *et al*: ALS-FTLD-linked mutations of SQSTM1/p62 disrupt selective autophagy and NFE2L2/NRF2 anti-oxidative stress pathway. Autophagy 16: 917-931, 2020.
46. Maiuri MC, Zalckvar E, Kimchi A and Kroemer G: Self-eating and self-killing: Crosstalk between autophagy and apoptosis. Nat Rev Mol Cell Biol 8: 741-752, 2007.
47. Su Z, Yang Z, Xu Y, Chen Y and Yu Q: Apoptosis, autophagy, necroptosis, and cancer metastasis. Mol Cancer 14: 48, 2015.
48. Fairlie WD, Tran S and Lee EF: Crosstalk between apoptosis and autophagy signaling pathways. Int Rev Cell Mol Biol 352: 115-158, 2020.
49. Cong L, Bai Y and Guo Z: The crosstalk among autophagy, apoptosis, and pyroptosis in cardiovascular disease. Front Cardiovasc Med 9: 997469, 2022.
50. Zhao WK, Zhou Y, Xu TT and Wu Q: Ferroptosis: Opportunities and challenges in myocardial ischemia-reperfusion injury. Oxid Med Cell Longev 2021: 9929687, 2021.
51. Zhang CX, Cheng Y, Liu DZ, Liu M, Cui H, Zhang BL, Mei QB and Zhou SY: Mitochondria-targeted cyclosporin A delivery system to treat myocardial ischemia reperfusion injury of rats. J Nanobiotechnology 17: 18, 2019.
52. Bugger H and Pfeil K: Mitochondrial ROS in myocardial ischemia reperfusion and remodeling. Biochim Biophys Acta Mol Basis Dis 1866: 165768, 2020.
53. Zhang Y, Wang Y, Xu J, Tian F, Hu S, Chen Y and Fu Z: Melatonin attenuates myocardial ischemia-reperfusion injury via improving mitochondrial fusion/mitophagy and activating the AMPK-OPA1 signaling pathways. J Pineal Res 66: e12542, 2019.
54. Cai Z, Li CF, Han F, Liu C, Zhang A, Hsu CC, Peng D, Zhang X, Jin G, Rezaeian AH, *et al*: Phosphorylation of PDHA by AMPK Drives TCA Cycle to promote cancer metastasis. Mol Cell 80: 263-278.e7, 2020.